Hysteretic nonlinear elasticity of Berea sandstone at low-vibrational strain revealed by dynamic acousto-elastic testing

G. Renaud,[1] J. Rivière,[2] P.-Y. Le Bas,[2] and P.A. Johnson[2]

Received 29 October 2012; revised 30 December 2012; accepted 7 January 2013; published 28 February 2013.

[1] Through changes in wave speed of ultrasonic pulses traversing the sample, we measure variations in the elasticity of dry Berea sandstone as a function of the applied low-frequency (LF) axial strain (varied from 10^{-7} to 10^{-5}). The approach, termed dynamic acousto-elasticity, is the dynamic analog of static acousto-elasticity where the wave speed is measured as a function of the applied static load. Dynamic acousto-elasticity uses low-frequency vibrational loading of smaller strain amplitude, typically below 10^{-4}, and it includes inertial effects. At strain amplitudes around 10^{-6}, compression and tension produce a material softening of the material. In contrast, a quasi-static compression inducing a strain between 10^{-4} and 10^{-3} leads to a material stiffening. At 10^{-5} strain amplitude, elaborate hysteretic signatures of modulus strain are observed. The measurements provide the first direct experimental evidence of hysteretic nonlinear (wave amplitude dependent) elasticity in a sandstone at low dynamic strains. **Citation:** Renaud, G., J. Rivière, P.-Y. Le Bas, and P. A. Johnson (2013), Hysteretic nonlinear elasticity of Berea sandstone at low-vibrational strain revealed by dynamic acousto-elastic testing, *Geophys. Res. Lett.*, *40*, 715–719, doi:10.1002/grl.50150.

1. Introduction

[2] It is well known that the elasticity of many isotropic solids, liquids, and gases can be described with a thermodynamic-based theory containing five constants, comprised of two linear moduli (λ and μ) and three nonlinear coefficients A, B, and C (Landau) or alternatively l, m, and n (Murnaghan) [*Guyer and Johnson*, 2009]. This elastic nonlinearity is termed quadratic because it corresponds to a term proportional to strain squared in the stress-strain relation, the equation of state. In Earth materials and damaged materials in general, quadratic elastic nonlinearity is not adequate to model experimental data; therefore, an additional term of higher-order proportional to strain cubed as well as a phenomenologic term that describes hysteresis in stress-strain are usually added in the equation of state [*Guyer et al.*, 1999; *Guyer and Johnson*, 2009]. It has been shown over the last decade that the elastic nonlinear behavior of Earth and damaged materials is amplitude dependent and that these materials show a transition from classical to hysteretic elastic as dynamic strain amplitudes increase [*Pasqualini et al.*, 2007]. The amplitude dependence has been explored applying Nonlinear Resonant Ultrasound Spectroscopy (NRUS) and other related methods that measure the average elastic behavior over multiple wave cycles [*Johnson et al.*, 1996]. The details of the elasticity over a single wave cycle are not captured with such methods. A robust method termed the Dynamic Acousto-Elasticity (DAE) has recently been developed for this purpose [*Renaud et al.*, 2011]. We recently reported [*Renaud et al.*, 2012a] the nonlinear elastic response of 11 dry rocks at two driving amplitudes (10^{-6} and 10^{-5} strain amplitudes) applying DAE.

[3] Development of DAE is important for application to characterizing the basic physics of Earth materials under dynamic forcing but also has many applications in the Earth. In the laboratory, the disturbance that induces elastic changes is a low-frequency wave at elevated strains (order 10^{-7}–10^{-5}), and the probe is a low-amplitude pulsed wave used to measure time delay changes, that is assumed not to disturb the material elastic behavior (the technique will be described in detail in the next section). In the Earth, the disturbance may be elastic change induced by fault slip, Earth tidal variations, barometric pressure, etc. The probe may be passive noise, repeating earthquakes, or active seismic sources. For example, applications include probing changes in local elastic properties preceding, during, and following slow and silent slip applying passive noise as has been done in the Guerrero region of Mexico [*Rivet et al.*, 2011]. Passive noise has also been used to probe crustal deformation post-earthquake, for instance following the 2004 M6.0 Parkfield earthquake [*Brenguier et al.*, 2008]. Other applications include extracting changes in elastic properties from interferometry applying ambient seismic noise at volcanoes, e.g., at Mt. Ruapehu, New Zealand during the 2006 eruption period [*Mordret et al.*, 2010] as well as application of repeating earthquake time delays to study elastic changes such as healing following the 2004 Parkfield event [*Li et al.*, 2006]. Applying a moving window cross-correlation technique of seismic waves [*Rubinstein et al.*, 2007] identified velocity changes caused by the Mw 8.0 2003 Tokachi-Oki earthquake near Hokkaido. Active seismic approaches are used to monitor near surface changes in velocity as well (e.g., *Silver et al.* [2007]), and solid Earth tide and barometric pressure induced elastic changes have been monitored applying passive seismic noise [*Wang et al.*, 2008]. While the above applications employ both dynamic and quasi-static perturbations, the methodologies are virtually the same. Our advancement in analysis will have import to all in situ applications.

[4] In this work, we present a detailed study of the influence of wave strain amplitude on the nonlinear elastic behavior of a room-dry Berea sandstone (Cleveland Quarries, Ohio),

[1]Department of Biomedical Engineering, Erasmus Medical Center, Rotterdam, The Netherlands.
[2]Earth and Environmental Sciences, Los Alamos National Laboratory, Los Alamos, NM, USA.

Corresponding author: G. Renaud, Department of Biomedical Engineering, Erasmus Medical Center, Rotterdam, The Netherlands. (renaud_gu@yahoo.fr)

0094-8276/13/10.1002/grl.50150

applying DAE at 13 different strain amplitudes ranging from 10^{-7} to 10^{-5}. We find that the elastic nonlinear response evolves with strain amplitude and that the nonlinear elastic parameters and hysteresis are wave amplitude dependent.

2. Dynamic Acousto-elastic Testing

2.1. Principle

[5] The purpose of DAE is to investigate the low-frequency (LF) nonlinear elastic behavior of a rock at a vibrational frequency of a few kHz by applying simultaneously a sequence of ultrasound (US) pulses [*Renaud et al*., 2011]. If the LF strain field traversed by the propagation path of the US pulses is quasi-homogeneous and quasi-static with regards to the US time of flight (TOF), then the progressive time delay of the US pulses allows one to measure variations in elasticity of the material under different strains, alternatively compressive and tensile. In order to accomplish this, a low-order compressional resonance mode of the rock sample is excited of which vibrational period is at least 10 times larger than the US TOF. The tensile response of rocks is generally neglected during quasi-static measurements partly because it is difficult to measure. The ability to measure both tension and compression elastic behavior of rocks is of great interest. In particular, it allows one to assess the equilibrium state of cracks; while closed cracks produce essentially no variation in elasticity during compression, partially closed cracks can induce a variation in elasticity under both tension and compression. Another advantage of DAE is the fact that the inertial regime is explored in contrast to the quasi-static regime. Inertia creates complexity in the nonlinear response not observed in the quasi-static regime.

[6] Here the low frequency is 4.5 kHz, selected to match the frequency of the lowest-order longitudinal resonance mode of the cylindrical sample (25 mm diameter and 150 mm length) of room-dry Berea sandstone. A heavy steel backload attached to the piezoelectric disc driving the LF excitation imposes fixed-free boundary conditions (Figure 1). Given these boundary conditions, a maximum strain is obtained near the fixed end of the sample, while the strain is zero near the free end of the sample. Thus, the selected resonance mode is such that the LF wavelength λ_{LF} equals 4 times the length of the sample L, $\lambda_{LF} = 4L$. In the geometry employed here, the US pulses are applied in a direction perpendicular to the LF wave. We position the US transducers close to the fixed end of the sample, where the LF strain is maximal. Consequently, the LF strain field is quasi-uniform along the US propagation path, i.e., the diameter of the sample. The US TOF is 10.2 μs (compressional velocity in dry Berea sandstone is 2450 m/s), and the LF wave period (222 μs) is more than 20 times larger; therefore, the LF strain is considered quasi-static during a US TOF. The LF axial strain undergone by the region of the sample probed by the US pulses is deduced from the acoustic particle velocity measured at the free end of the sample by a laser Doppler vibrometer (Polytec Inc., USA) where the LF displacement is maximum (Figure 1). Two disc-shaped 6 mm diameter US piezoelectric transducers (Olympus Inc., USA) are used to generate and receive pulses in the frequency range 1–2 MHz. Coupling gel is applied between the sample and transducers. A thin layer of nail polish is placed on the contact area so that the gel does not penetrate through the rock via capillary action. A US pulse produces a maximum strain amplitude of the order of 10^{-7} (measured in a separate experiment with a laser Doppler vibrometer). Grain size in Berea sandstone is typically 100 to 200 micrometers [*Guyer and Johnson*, 2009]. The wavelength is of the order of 0.55 m at 4.5 kHz, while it is close to 2 mm for ultrasonic frequencies in the range 1–2 MHz. Therefore, the wavelength of the US pulses is at least 10 times larger than the grain size of the sample.

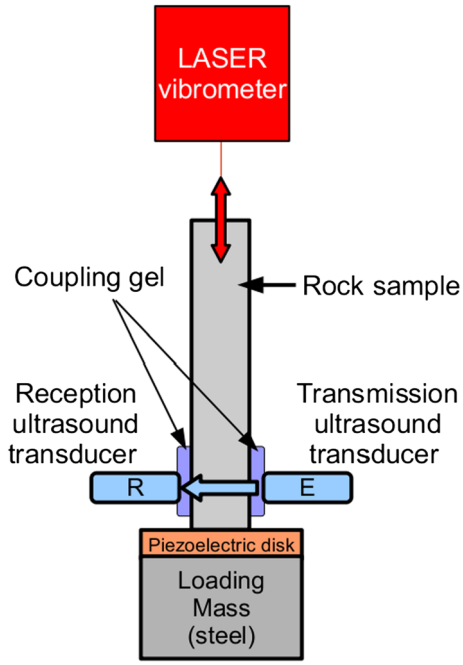

Figure 1. Experimental setup to perform dynamic acousto-elastic testing.

2.2. Signal Processing

[7] For each US pulse, we calculate the variation in the elastic modulus M derived from the variation in the propagation velocity V of compressional US waves (see *Renaud et al*. [2012a] for more details), since $M = \rho V^2 = \lambda + 2\mu$ where ρ is the density of the material and λ and μ are the second-order elastic constants of Lamé. Each successive US pulse is associated with the axial LF strain ε_{LF} experienced by the material during its TOF in the sample. This procedure is applied over many wave cycles so that the LF strain is extremely well sampled. The synchronization of the LF and US signals allows one to relate $(M(\varepsilon_{LF}) - M_0)/M_0$ with ε_{LF} during the steady state of the LF resonance when a stable LF strain amplitude is reached. M_0 is the value at equilibrium, in the absence of the LF excitation. The variations in M measured in dry rocks consist of an offset and a fast modulation at the frequency of the LF resonance [*Renaud et al*., 2011; *Renaud et al*., 2012a].

[8] The elastic nonlinearity measured in Earth materials is complex due to hysteresis and material conditioning/relaxation effects, and modeling these behaviors is challenging [*Scalerandi et al*., 2010]. Conditioning is the phenomenon whereby the material modulus diminishes progressively with time under excitation by a dynamic wave. Relaxation in the form of slow dynamics follows when the wave excitation is terminated. There exist physics-based theoretical approaches, such as Arrhenius-like models [*Gusev and Tournat*, 2005] as well as phenomenologic theories, e.g., the Preisach theory

[*Guyer et al.*, 1995; *Guyer and Johnson*, 2009]. Rather than appeal to theories that contain hysteresis, we currently apply a practical approach that allows us to simplify the analysis but nonetheless determine the approximate quadratic and cubic nonlinear parameters. We extract parameters as a function of the LF strain by applying a second-order polynomial fit: $\Delta M(\varepsilon_{\mathrm{LF}})/M_0 \approx C_E + \beta_E \varepsilon_{\mathrm{LF}} + \delta_E \varepsilon_{\mathrm{LF}}^2$, where β_E and δ_E are the classical nonlinear elastic parameters for quadratic and cubic elastic nonlinearities, respectively [*Johnson et al.*, 1996]. C_E quantifies the offset of the variation in M due to nonlinear material conditioning [*TenCate*, 2011; *Renaud et al.*, 2011]. β_E and δ_E are defined for materials exhibiting classical nonlinear behavior due to anharmonicity [*Landau and Lifshitz*, 1986; *Zarembo and Krasil'nikov*, 1971]. While the elastic nonlinearity in rock is dominated by material damage in the form of cracks ranging from nanoscale to millimeter scale and potentially other features, the classical nonlinear description can still provide insight and serve as the basis for comparison with other materials.

3. Metastable Elastic Nonlinear Responses of Berea Sandstone

3.1. Dynamic Variations in Elasticity Induced by an LF Strain

[9] In this section, we show the variations in the elastic modulus induced by the LF axial strain as measured by DAE. The measurement was performed for 13 different axial LF strain amplitudes, ranging from 10^{-7} to 10^{-5} (Figure 2). A positive axial LF strain corresponds to a tensile axial strain, while a negative axial LF strain represents a compressive axial strain. The material conditioning induced by the LF dynamic wave corresponds to a net decrease in the modulus as a function of strain amplitude. The relative compression/tension oscillate about this metastable state. For LF strain amplitudes between 5×10^{-7} and 2×10^{-6}, both axial compression and axial tension produce a softening of the material. As dynamic strain reaches 10^{-5}, the material evolves to exhibiting softening under tension while globally stiffening under compression. However, even until a strain amplitude of 10^{-5}, the beginning of the compressive phase (from strain 0 to -2×10^{-6}) produces a decrease in the elastic modulus. The corresponding decreasing rate (equivalent to a local value of the nonlinear parameter β_E calculated between strain 0 and -2×10^{-6}) is of the order of 10^2 and appears to be conserved for all strain amplitudes investigated here. In addition, when increasing the LF strain amplitude, we observe a progressive increase in hysteresis. Hysteretic loops appear both in compression and in tension. Note that the LF strain also produces a modulation of ultrasound attenuation [*Renaud et al.*, 2011; *Renaud et al.*, 2012a]. Here we focus on the effect of the LF strain on elasticity.

[10] A softening at the beginning of the compressive phase from strain 0 to -1×10^{-6} was also observed in four other room-dry sandstones applying DAE [*Renaud et al.*, 2012a]. This decrease in elastic modulus is contrary to expectations from the static point of view, since an increase in elastic modulus (or increase in wave speed) occurs when pre-existing cracks are closed by increasing moderate compressive stress (strains between 10^{-4} and 10^{-3}), as observed during quasi-static acousto-elastic testing [*Winkler and McGowan*, 2004] and quasi-static stress-strain measurement [*Vakhnenko et al.*, 2007]. However, under quasi-static stress cycling with fixed average stress (overburden stress), quasi-static modulus softening is also observed as the quasi-static strain amplitude increases [*Tutuncu et al.*, 1998]. In summary, both dynamic (this study) and quasi-static stress cycling produce modulus softening.

[11] Quasi-static measurements in Berea sandstone [*Tutuncu et al.*, 1998; *Winkler and McGowan*, 2004; *Vakhnenko et al.*, 2007] differ from our DAE experiments in the strain applied but also in the strain rate. In this study, the material experiences strain rates between 10^{-3} s^{-1} and 10^{-1} s^{-1}, while the rock is subjected to lower strain rates in the range 10^{-6} s^{-1} – 10^{-3} s^{-1} in quasi-static measurements. Thus, differences in strain and strain rate may also explain discrepancies (in particular, the compression behavior) observed between

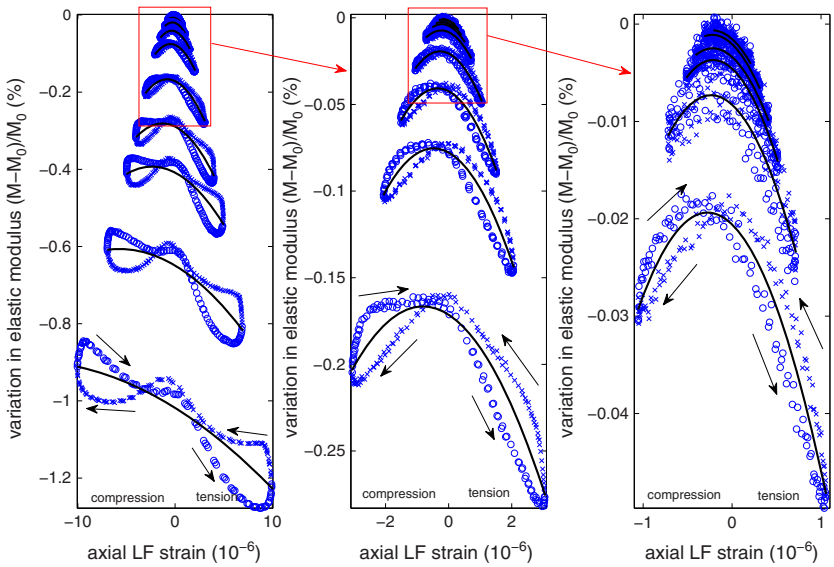

Figure 2. Variation in the elastic modulus as a function of the axial LF strain at 13 different LF strain amplitudes from 10^{-7} to 10^{-5}. Solid lines show the second-order polynomial fit described in the text. Circles and crosses indicate increasing and decreasing LF strain, respectively.

our dynamic measurements of nonlinear elasticity and reported quasi-static measurements. A last difference is that our measurements explore the dynamic behavior about the equilibrium state of the rock; in particular, the tensile response is not investigated by quasi-static experiments since an overburden stress is always applied.

3.2. Dependence of Nonlinear Parameters on the LF Strain Amplitude

[12] Figure 3 shows the amplitude dependence of nonlinear parameters. As the LF strain amplitude increases, β_E and C_E increase in absolute value, whereas δ_E decreases in absolute value. This observation is not what one expects in undamaged homogeneous materials such as mono-crystalline metals or polymers for which nonlinear elastic parameters are not wave amplitude dependent. A similar amplitude dependence of nonlinear parameters was also observed in a previous study conducted in Lavoux limestone [*Renaud et al*., 2011; *Renaud et al*., 2012b].

3.3. Effect of Material Conditioning

[13] Careful measurements in sandstones applying NRUS [*Pasqualini et al*., 2007; *TenCate*, 2011] showed three elastic regimes: (i) linear elasticity, (ii) classical nonlinear elasticity (resonance frequency shift proportional to the squared driving amplitude) with no conditioning, and (iii) a regime showing non-classical nonlinear elasticity (power law relating the resonance frequency shift to the driving amplitude with a scaling exponent of approximately 1) with conditioning. In DAE, nonlinear material conditioning is quantified by the offset C_E. Here it increases from 10^{-5} to 10^{-2} as the LF strain amplitude increases (Figure 3). The

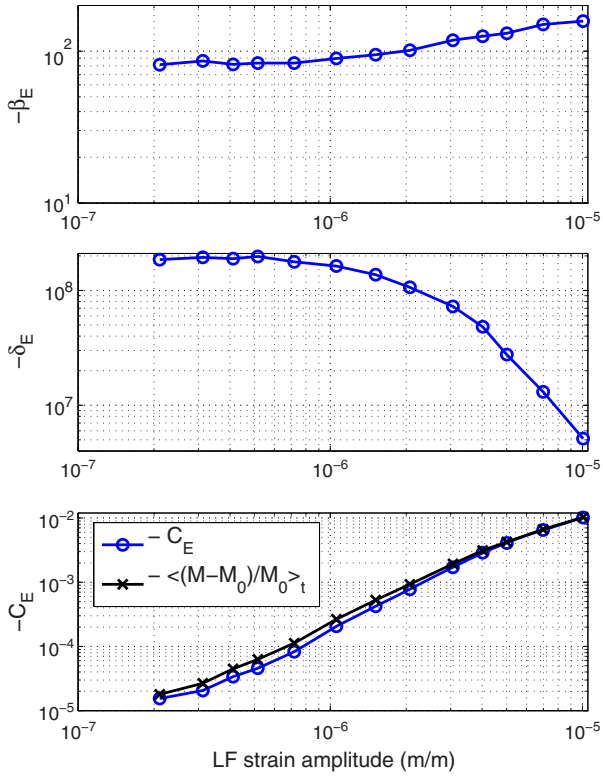

Figure 3. Nonlinear parameters and the time-averaged variation in elasticity $<\frac{\Delta M(\varepsilon_{LF})}{M_0}>_t$ measured in Berea sandstone as functions of the axial LF strain amplitude.

work by *Pasqualini et al*. [2007] reports that the transition between the classical nonlinear regime (ii) and the nonlinear/hysteretic regime (iii) occurs in a range of strain amplitude between 10^{-7} and 10^{-6} in room-dry sandstones. At this transition, *Pasqualini et al*. [2007] show that conditioning commences. In that work and the work of others, conditioning was manifest by a decrease in elastic modulus during wave excitation, which recovers slowly back to the rest (M_0) state (the slow dynamics). We note that in these and nearly all other measurements on rock, the probe of the elasticity is also the waveform inducing the change (the "pump"). In DAE, we have the advantage of a separate probe and pump wave. Our measurements suggest that the onset of regime (iii) appears at a LF strain amplitude close to 10^{-7}, corroborating the results by *Pasqualini et al*. [2007]. Finally, we observe that conditioning brings the material to a metastable state, different for each LF strain amplitude, and modifies the fast nonlinear elastic behavior. Interestingly, the time-averaged variation in M over one acoustic cycle increases as the LF strain amplitude increases, and it is primarily due to the increase in C_E produced by conditioning. At low strain amplitudes ($<2\times10^{-6}$), cubic nonlinearity quantified by δ_E contributes to the time-averaged variation in M, so it slightly exceeds the value of C_E. But δ_E decreases as the LF strain amplitude increases (Figure 3), so the time-averaged variation in M is solely produced by material conditioning for LF strain amplitudes higher than 2×10^{-6}.

3.4. Hysteretic Nonlinear Elasticity

[14] The application of the classical formulation (Figure 3) does not capture the hysteresis exhibited by the nonlinear elastic response of Berea sandstone (Figure 2). In a previous study [*Renaud et al*., 2012b], we showed that the importance of hysteresis in the nonlinear elastic behaviors measured by DAE can be quantified by a double integration of $\Delta M(\varepsilon_{LF})$ with respect to ε_{LF}. The first integration provides a dynamic stress-strain relation, and a second integration over a LF wave cycle provides an estimate of energy loss due to hysteretic nonlinear elasticity. For each LF strain amplitude ε_{LFAmpl}, we calculated the energy loss per acoustic cycle $\frac{\Delta E}{E_0}$, with $\Delta E = \oint \sigma d\varepsilon$ and $E_0 = M_0\varepsilon^2_{LFAmpl}$. As a result, the variation in the inverse quality factor Q^{-1} due to hysteretic nonlinear elasticity can be estimated since $Q^{-1} = \frac{\Delta E}{2\pi E_0}$. Figure 4 shows that the variation in Q^{-1} increases as the axial LF strain amplitude increases. This provides for the first time direct evidence of the amplitude dependence of hysteretic nonlinear elasticity in a sandstone in this strain range. Although stress-strain hysteresis was reported applying quasi-static mechanical testing, it was speculated to appear also at low dynamic strains, below 10^{-4}, based on the observation of non-classical behaviors by applying NRUS or by studying waveform distortion [*Guyer and Johnson*, 2009]. In contrast and of interest is that no wave amplitude dependence of hysteresis was measured in dry Lavoux limestone applying DAE [*Renaud et al*., 2012b]. The two differing results suggest strong differences in the elasticity of different Earth materials.

[15] Amplitude dependence of Q^{-1} was reported applying NRUS in a similar experimental configuration where an axial compressional resonance mode of a cylindrical rod is excited [*Guyer et al*., 1999]. The variation in Q^{-1} (Figure 4)

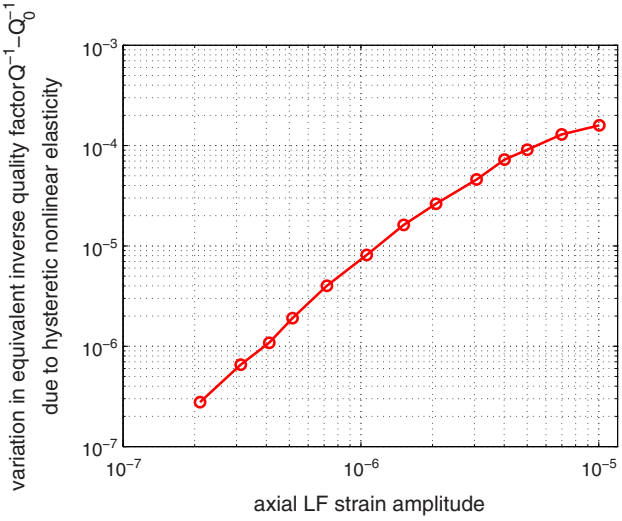

Figure 4. Variation in equivalent inverse quality factor as a function of the axial LF strain amplitude. The amplitude dependence is attributable to stress-strain hysteresis.

and the time-averaged variation in M (Figure 3) introduced in this study cannot be directly compared to these NRUS measurements. This is due to the anisotropy of the acousto-elastic effect when a uniaxial strain is applied to an isotropic solid [*Renaud et al*., 2012b]. Based on the third-order elastic constants A, B, and C measured by quasi-static acousto-elastic testing [*Winkler and McGowan*, 2004], the scaling factor between variations in elasticity (deduced from variations in wave speed) measured perpendicular and parallel to the uniaxial loading is close to 10 for dry Berea sandstone. Therefore, variations in elasticity could be expected to be 10 times higher along the axis of the uniaxial loading. This suggests that applying NRUS in the same experimental configuration (Figure 1) would measure variations in Q^{-1} due to hysteretic nonlinear elasticity an order of magnitude higher than values reported in Figure 4.

[16] Work is ongoing to study the consistency of the characterization of elastic nonlinearity provided by NRUS and DAE. We neglected the possible mutual interaction between the US pulses and the LF vibration in a medium exhibiting hysteretic nonlinear elasticity [e.g., *Zaitsev et al*., 2005]; this issue will be addressed in future studies.

4. Summary

[17] Applying dynamic acousto-elastic testing, the metastable nonlinear elastic behavior of room-dry Berea sandstone was measured at 13 different strain amplitudes, ranging from 10^{-7} to 10^{-5}. At LF strain amplitudes around 10^{-6}, both axial compression and axial tension produce a softening of the material, in contrast to the effect of a quasi-static compression. At higher LF strain amplitudes, elaborate nonlinear and hysteretic signatures of modulus strain are observed. Finally, direct evidence of dynamic hysteretic nonlinear elasticity was observed. A long-term goal is to identify the physical mechanisms responsible for the observed elastic nonlinear behaviors of Earth materials and to evaluate the influence of external static pressure and a saturating fluid. Another goal is to refine the data processing technique for in situ applications. The DAE methodology should have broad application to in situ measures of elastic change induced by earth tides, slow and silent slip or post slip relaxation.

[18] **Acknowledgments.** We gratefully acknowledge the support of the U. S. Department of Energy, Office of Basic Energy Research. The authors thank Ton van der Steen (Erasmus Medical Center, Rotterdam, The Netherlands). We also thank T. J. Ulrich, and J. A. TenCate for discussions and experimental assistance, and Robert Guyer for discussions.

References

Brenguier, F., M. Campillo, C. Hadziioannou, N. Shapiro, R. Nadeau, and E. Larose (2008), Postseismic relaxation along the San Andreas fault at Parkfield from continuous seismological observations, *Science*, *321*(5895), 1478–1481.

Gusev, V., and V. Tournat (2005), Amplitude- and frequency-dependent nonlinearities in the presence of thermally-induced transitions in the Preisach model of acoustic hysteresis, *Phys. Rev. B*, *72*, 054,104,1–19.

Guyer, R., and P. Johnson (2009), *Nonlinear Mesoscopic Elasticity*, 1–396 pp., Wiley-VCH Verlag GmbH & Co. KGaA, Weinheim, Germany.

Guyer, R., K. McCall, and G. Boitnott (1995), Hysteresis, discrete memory and nonlinear wave propagation in rock: A new paradigm, *Phys. Rev. Lett.*, *74*, 3491–3494.

Guyer, R., J. TenCate, and P. Johnson (1999), Hysteresis and the dynamic elasticity of consolidated granular materials, *Phys. Rev. Lett.*, *82*(16), 3280–3283.

Johnson, P., B. Zinszner, and P. Rasolofosaon (1996), Resonance and elastic nonlinear phenomena in rock, *J. Geophys. Res.*, *101*(B5), 11,553–11,564.

Landau, L., and E. Lifshitz (1986), *Theory of Elasticity—Third Edition* (Course of Theoretical Physics, Volume 7), 1–195 pp., Butterworth-Heinemann, Oxford.

Li, Y.-G., P. Chen, E. Cochran, J. Vidale, and T. Burdette (2006), Seismic evidence for rock damage and healing on the San Andreas fault associated with the 2004 m 6.0 Parkfield earthquake, *Bull. Seismol. Soc. Am.*, *96*(4B), S349–S363.

Mordret, A., A. Jolly, Z. Duputel, and N. Fournier (2010), Monitoring of phreatic eruptions using interferometry on retrieved cross-correlation function from ambient seismic noise: Results from Mt. Ruapehu, New Zealand, *J. Volcanol. Geotherm. Res.*, *191*(1–2), 46–59.

Pasqualini, D., K. Heitmann, J. TenCate, S. Habib, D. Higdon, and P. Johnson (2007), Nonequilibrium and nonlinear dynamics in Berea and Fontainebleau sandstones: Low-strain regime, *J. Geophys. Res.*, *112*(B1), 1–16.

Renaud, G., M. Talmant, S. Callé, M. Defontaine, and P. Laugier (2011), Nonlinear elastodynamics in micro-inhomogeneous solids observed by head-wave based dynamic acoustoelastic testing, *J. Acoust. Soc. Am.*, *130*(6), 3583–3589.

Renaud, G., P.-Y. Le Bas, and P. Johnson (2012a), Revealing highly complex elastic nonlinear (anelastic) behavior of earth materials applying a new probe: Dynamic acoustoelastic testing, *J. Geophys. Res.*, *117*(B6), 1–17.

Renaud, G., J. Rivière, S. Haupert, and P. Laugier (2012b), Anisotropy of dynamic acoustoelasticity in limestone, influence of conditioning and comparison with nonlinear resonance spectroscopy, *accepted in J. Acoust. Soc. Am.*.

Rivet, D., M. Campillo, N. Shapiro, V. Cruz-Atienza, M. Radiguet, N. Cotte, and V. Kostoglodov (2011), Seismic evidence of nonlinear crustal deformation during a large slow slip event in Mexico, *Geophys. Res. Lett.*, *38*(8), L08308.

Rubinstein, J., N. Uchida, and G. Beroza (2007), Seismic velocity reductions caused by the 2003 Tokachi-Oki earthquake, *J. Geophys. Res.*, *112*(B5), B05315.

Scalerandi, M., A. Gliozzi, C. Bruno, and P. Antonaci (2010), Nonequilibrium and hysteresis in solids: Disentangling conditioning from nonlinear elasticity, *Phys. Rev. B*, *81*, 104,114.

Silver, P., T. Daley, F. Niu, and E. Majer (2007), Active source monitoring of cross-well seismic travel time for stress-induced changes, *Bull. Seismol. Soc. Am.*, *97*(1B), 281–293.

TenCate, J. (2011), Slow dynamics of earth materials: An experimental overview, *Pure Appl. Geophys.*, pp. 1–9.

Tutuncu, A., A. Podio, A. Gregory, and M. Sharma (1998), Nonlinear viscoelastic behavior of sedimentary rocks, part I: Effect of frequency and strain amplitude, *Geophysics*, *63*(1), 184–194.

Vakhnenko, V., O. Vakhnenko, J. TenCate, and T. Shankland (2007), Modeling of stress-strain dependences for Berea sandstone under quasistatic loading, *Phys. Rev. B*, *76*, 184,108.

Wang, B., P. Zhu, Y. Chen, F. Niu, and B. Wang (2008), Continuous subsurface velocity measurement with coda wave interferometry, *J. Geophys. Res.*, *113*(B12), 313.

Winkler, K., and L. McGowan (2004), Nonlinear acoustoelastic constants of dry and saturated rocks, *J. Geophys. Res.*, *109*, B10,204.

Zaitsev, V., V. Gusev, and Y. Zaytsev (2005), Mutually induced variations in dissipation and elasticity for oscillations in hysteretic materials: Non-simplex interaction regimes, *Ultrasonics*, *43*, 699–709.

Zarembo, L., and V. Krasil'nikov (1971), Nonlinear phenomena in the propagation of elastic waves in solids, *Sov. Phys. Usp.*, *13*(6), 778–797.